Reduction of Structure-Borne Noise in Automobiles by Multivariable Feedback

M.-P. Jolicoeur, J.-G. Roumy, S. Vanreusel, D. Dionne, H. Douville, B. Boulet, *Member, IEEE,* H. Michalska, *Member, IEEE,* P. Masson, and A. Berry

Abstract— **The vibration transmitted through the suspension of a car is the dominant source of structurally-generated interior noise at low frequencies. With the addition of actuators between the suspension attachment points and the car frame, we propose the design of a feedback controller for an active control of the vibrations to reduce cabin noise. A model-based controller design requires the identification of a transfer function model of the suspension, the frame, and the cabin acoustics. Here we deal with model identification of a suspension testbed. Uncertainty bounds for the flexible mode parameters of the model are estimated from experimental input-output data for a future robust mu-synthesis controller design. A preliminary controller is designed and tested by simulation for the identified nominal model. Inputs to the controllers are given by force and acceleration sensors measuring the vibration at different points on the suspension.**

I. Introduction

Many sources contribute to the ambient noise inside the passenger cabin of an automobile, such as the engine or air ducts. However, the principal source of low frequency noise is the road-induced vibration that propagates as structure-borne sound. Hermans and Van Der Auweraer [1] demonstrated it by taking structural and acoustical measurements inside an automobile, and identified the main source of the noise as road-induced vibrations causing a resonance. Similarly, Kim, Lee and Sung [2] found that car interior noise is caused in the low-frequency range by modal characteristics of the structure such as acoustic resonances, body vibration modes and structural-acoustic coupling characteristics.

A noticeable reduction in the perceived level of noise can therefore be achieved by performing an active control of vibrations. Stobener and Gaul [3] implemented a modal controller by installing an array of piezoelectric sensors on the floor and centre panel of the body, with good results.

This paper investigates the effectiveness of feedback-controlled actuators placed directly on the suspension, thus reducing the transmission of vibrations to the frame. A modal analysis is performed on a one-wheel car suspension to identify a model with parametric uncertainty bounds with the objective of designing a robust controller. A preliminary feedback controller designed using the H_∞ control technique, which has been used in vibration control problems [4, 5], is showing some promise by providing more damping to the flexible modes of the suspension testbed.

Manuscript received February 28, 2005.

M.-P. Jolicoeur, J.-G. Roumy, S. Vanreusel, D. Dionne, B. Boulet, H. Michalska are with the McGill Centre for Intelligent Machines, Montreal, Quebec, Canada (phone: 514-398-1478; fax: 514-398-7348; e-mail: boulet@cim.mcgill.ca).

H. Douville, P. Masson, and A. Berry are with the GAUS Laboratory, Université de Sherbrooke, Québec, Canada.

II. Model Identification

The car suspension testbed can be modeled in terms of its modes of vibration. A finite-element model (FEM) would be difficult to obtain, and might yield poor results in view of the complexity of the suspension structure. Therefore, a more direct way to obtain a dynamic model in this case is to use experimentally acquired data in a system identification procedure.

Figure 1 shows the one-wheel car suspension experimental testbed at the GAUS laboratory at Université de Sherbrooke. A shaker is attached to the wheel axle to simulate the road disturbance, and a force sensor records the force applied to the axle. Different acceleration and force sensors are placed on the suspension attachment points to record its behavior when excited. Figure 2 shows the location and denomination of the suspension attachment points to the car frame. Four three-axis (x, y and z) accelerometers are placed at the suspension base's attachment points (B1, B2, B3 and B4). Three force sensors are placed at the top of the suspension (Bh) in all three axes. The suspension is excited through the shaker with white Gaussian noise for a period of six seconds during which sensor information is recorded at a sampling frequency of 1000 Hz. The type of force sensor used gives a value that is proportional to the displacement.

A. FRF Computation

The frequency response functions (FRF) represent, for each sensor, the ratio of the output Fourier transform $X(\omega)$ over the input Fourier Transform $F(\omega)$.

$$H(\omega) = \frac{X(\omega)}{F(\omega)} \tag{1}$$

In an experimental environment, two FRFs denoted $H_1(\omega)$ and $H_2(\omega)$ are obtained. FRF $H_1(\omega)$ is defined as the cross-spectrum of the input and output signals divided by the energy spectral density of the input, whereas $H_2(\omega)$ is the energy spectral density of the output divided by the cross-spectrum of the input and output signals. These FRFs should be identical in theory [6]. However, they typically differ due to physical constraints such as noise on the input or the output sensor signal, nonlinearities on the structure or finite sampling. Due to the way they are computed [7, 8], $H_2(\omega)$ is likely more accurate near a resonance, while $H_1(\omega)$ is a better approximation of the system response around an antiresonance. The coherence function defined as $\gamma^2(\omega) := H_1(\omega)/H_2(\omega) \le 1$, provides a means of quantifying the uncertainty on the FRFs. A value inferior to 1.0 denotes a discrepancy between $H_1(\omega)$ and $H_2(\omega)$, and indicates the presence of noise. Generally, a coherence value above 0.9 is considered good.

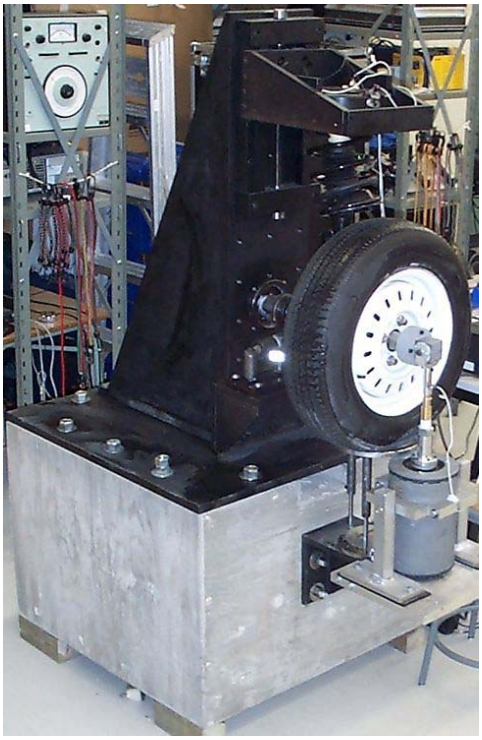

Figure 1 - Experimental test bench at Université de Sherbrooke

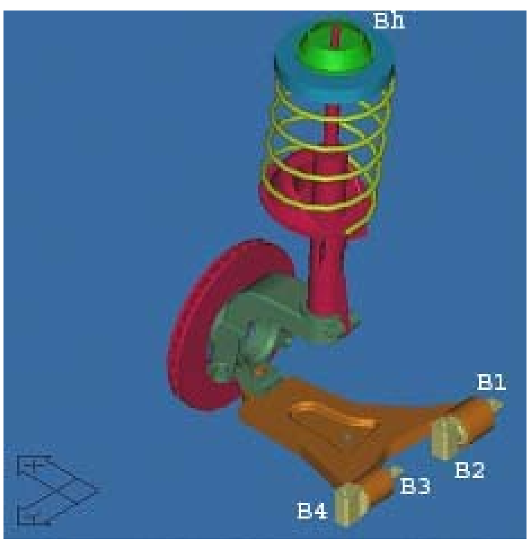

Figure 2 - Sensor location on the suspension

B. Data Selection

To control the vibrations transmitted through the suspension, a model that is accurate in the vicinity of the system's resonant frequencies is desirable. Thus, $H_2(\omega)$ represents a better choice. Figure 3 represents the H, H_1 and H_2 FRFs computed from the data of the *x*-direction accelerometer placed at B1 and Figure 4 the corresponding coherence function. The frequency range of interest is 20Hz to 160Hz because the coherence is good and the resonance peaks in this range are generated by the dynamical properties of the suspension as determined experimentally.

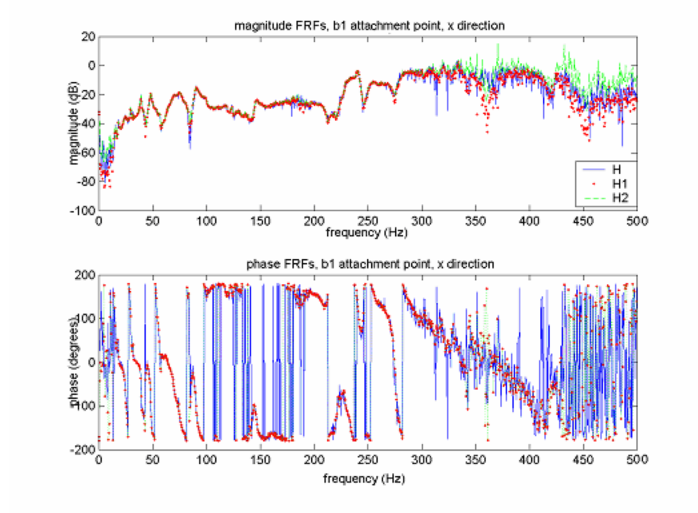

Figure 3 - Sample FRF showing H, H1 and H2

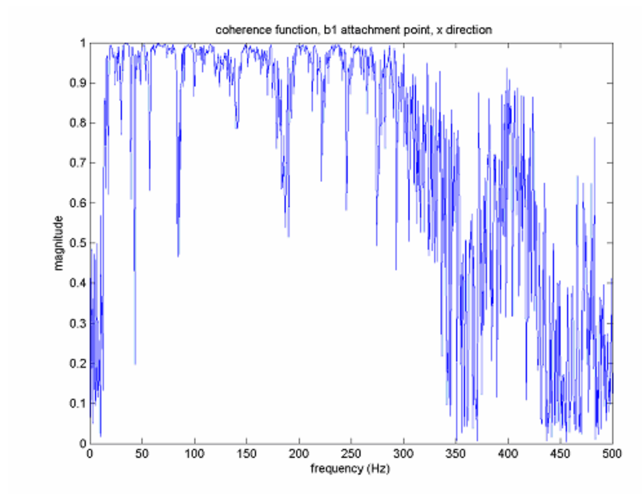

Figure 4 - Sample Coherence function

C. Identification of Modal Parameters

The structure's modal parameters ω_n and ζ are identified through curve fitting. The method used is the so-called Multiple Degrees of Freedom (MDOF) and implies finding simultaneously all the parameters of the transfer function describing a particular FRF.

The FRFs measured at the base of the suspension are acceleration over force, called accelerance FRFs. The FRFs measured at the head of the suspension are force over force, but as mentioned earlier in this case the force output is proportional to the displacement, therefore these FRFs can be considered as receptance FRFs and the receptance equation can be used to model them.

n-DOF accelerance FRFs can be modeled using a parallel interconnection of second-order transfer functions. A_i represents the gain factor from the i[th] input to the output.

$$H(\omega)=\sum_{i=1}^{n}\frac{-A_i\omega^2}{\omega_{ni}^2-\omega^2+2j\zeta_i\omega_{ni}\omega} \quad (2)$$

Similarly, *n*-DOF receptance FRFs can be modeled using the equation:

$$H(\omega)=\sum_{i=1}^{n}\frac{A_i}{\omega_{ni}^2-\omega^2+2j\zeta_i\omega_{ni}\omega} \quad . \quad (3)$$

The number of terms in the summation (representing the Degrees of Freedom) is selected by visual inspection of the experimental FRFs. There must be enough DOFs to properly model all significant vibration modes of the structure, yet the model has to be of a low enough order so that it is manageable for numerical purposes.

The structure's principal resonant modes are identified by adding all FRFs together as shown in Figure 5. Since the resonances are present on all FRFs, the real peaks are amplified and the false peaks, which may be due to noise and are therefore different on each FRF, are eliminated. Despite adding all the FRFs, it can be shown that certain modes which appear real are not part of the structure, such as the peak around 83 Hz on Figure 5.

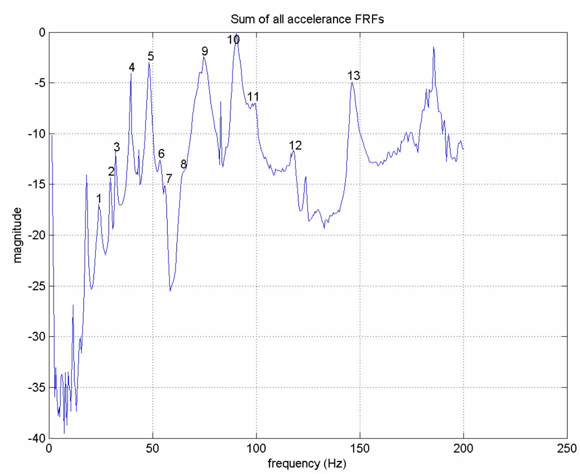

Figure 5 - Sum of the acceleration/force FRFs

This peak can be traced to a single data point on one FRF and does not appear on any other FRF. After careful consideration of all the data available, it is possible to distinguish 13 modes in the frequency range 20 Hz to 160 Hz. The mode around 185 Hz on Figure 5 has been traced back to the tire, and therefore will not be part of the suspension model.

D. Frequency Response Fitting Algorithm

The transfer function coefficients for each of the 13-DOF FRFs are determined using the Matlab Curve Fitting Toolbox using a robust least squares algorithm [9].

Figure 6 shows a sample curve fitting for a receptance FRF. Throughout this paper, the output from the sensor located at the head of the suspension in the z direction is used to illustrate the statements being made, as the most significant forces are exerted at this location. Each mode's damping ratio and natural frequency, shown in Table 1, are computed from the average of the 15 values determined during the curve fit. A second iteration of the curve-fitting algorithm is necessary to find the gain values corresponding to the fixed modal parameters.

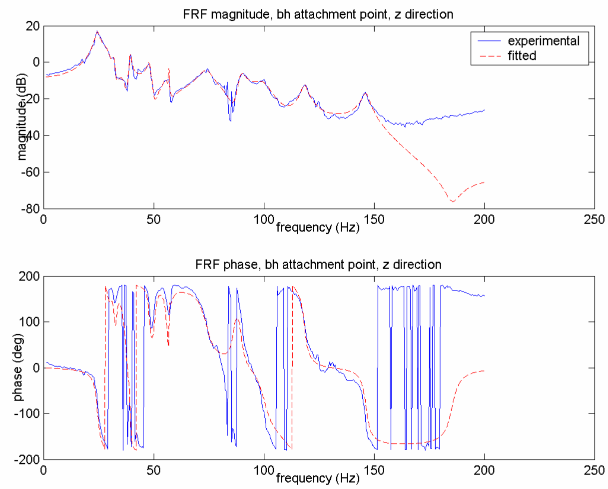

Figure 6 - Fit performed on the FRF taken at bh, z direction

Table 1 – vibration modes of the ¼ car suspension

Mode	Frequency (Hz)	Damping (%)
1	24.26	4.41
2	30.00	1.46
3	32.26	1.68
4	39.49	1.68
5	48.44	2.37
6	54.31	1.49
7	56.56	1.16
8	63.49	2.67
9	74.89	3.20
10	90.14	1.60
11	100.3	1.91
12	118.4	0.83
13	145.9	1.27

E. Uncertainty Modeling

In this section, we address the problem of characterizing the level of uncertainty in the modal parameters given the experimental FRFs, and a nominal modal as a seed for the algorithm. What is needed for robust control design is a set of tight bounds on the modal parameters of the nominal model defining a family of models from which one can basically reproduce all the input-output data. The receptance function is used as an example.

$$H(j\omega)=\frac{A}{\omega_n{}^2-\omega^2+2j\zeta\omega_n\omega} \quad (4)$$

The objective is to define uncertainty bounds on the modal parameters ω_n, ζ and A. The frequency response with parametric uncertainty becomes

$$H(j\omega)=\frac{(A+\Delta A)}{(\omega_n+\Delta\omega_n)^2-\omega^2+2j(\zeta+\Delta\zeta)(\omega_n+\Delta\omega_n)\omega} \tag{5}$$

With a set of bounds, it is possible to generate an infinite set of perturbed models. This family of perturbed models is

$$\mathcal{F}:=\left\{F(j\omega)=\frac{(A+\Delta A)}{(\omega_n+\Delta\omega_n)^2-\omega^2+2j(\zeta+\Delta\zeta)(\omega_n+\Delta\omega_n)\omega}: \left|\Delta\omega_n\right|\le\Delta\omega_{n\ \max},\ \left|\Delta\zeta\right|\le\Delta\zeta_{\max},\ \left|\Delta A\right|\le\Delta A_{\max}\right\} \tag{6}$$

The goal is to define the set $\mathcal{F}$ so it can contain every possible behavior of the physical system denoted as $\mathcal{P}$. Hence, $\mathcal{P}$ should be a subset of $\mathcal{F}$. Proving the latter relationship would ensure that the uncertainty bounds are adequate. However, this is impossible to prove as $\mathcal{P}$ is unknown, except for a set of experimental data obtained from the physical system. Even if $\mathcal{P}$ were known, ensuring that all possible frequency responses are included in the set of perturbed models might require large uncertainty bounds to account for unmodeled dynamics which would significantly reduce the performance of the robust controller. A more realistic objective is to show that the family of perturbed models $\mathcal{F}$ may reproduce all available experimental frequency responses $\mathcal{E}$, to within some tolerance.

In reality, the experimental frequency responses may only be compared to a finite subset of $\mathcal{F}$. This subset is obtained by discretizing the uncertainty intervals (frequency gridding also reduces the subset further.) For example, if the value of the nominal gain is 0.24 with an uncertainty bound of ±1%, a step of 0.5% may be used to obtain 5 possible values for the gain {-0.2424, -0.2412, 0.0000, 0.2412, 0.2424}. This is repeated for all parameters. Finally, the responses for all combinations of parameters are computed. Since only a finite subset of $\mathcal{F}$ is used, it becomes impossible to find perfect matches between the experimental responses and the sampled perturbed responses. The proposed solution is as follows. All sampled perturbed responses $F_k(j\omega)$ are compared to the experimental response $E_i(j\omega)$. The error between $E_i(j\omega)$ and each $F_k(j\omega)$ is computed using the 1-norm.

$$\text{error} \ = \ \left\| E_i(j\omega)-F_k(j\omega)\right\|_1 \tag{7}$$

This error is then minimized. The best $F_k(j\omega)$ for which the error is minimized is denoted as $F_k(j\omega)^b$. A trial and error method is used for the minimization.

$$\begin{aligned}&\min\ \left\| E_i(j\omega)-F_k(j\omega)\right\|_1\\ &k=1,\dots,K\end{aligned} \tag{8}$$

K : number of combinations

Using the 1-norm for the error is equivalent to using the mean error over all frequencies. It ensures that the error is minimized over all modes. It is preferred over the infinity-norm, which is equivalent to the maximum error. Using the maximum error often gives unsatisfactory results, as it may tend to minimize the error in problematic frequency bands only. The procedure used to define the uncertainty bounds for one experimental response $E_i(j\omega)$ is the following:

- Bounds are initially defined on the modal parameters.
- $F_k(j\omega)^b$ is selected within the family of models defined by these bounds.

The minimized error is evaluated to establish if it is small enough to indicate that $E_i(j\omega)$ is in fact close enough to $F_k(j\omega)$. If not, then the uncertainty bounds on the modal parameters are increased and the steps above are repeated until a suitable error is obtained for $E_i(j\omega)$. Once the error is acceptable, the variations on the parameters that are used to obtain $F_k(j\omega)^b$ are noted.

$$F_k(j\omega)^b:=\left\{\frac{(A+\Delta A)}{(\omega_n+\Delta\omega_n)^2-\omega^2+2j(\zeta+\Delta\zeta)(\omega_n+\Delta\omega_n)\omega}: \Delta\omega_n=\Delta\omega_{n\ \exp i}*,\ \Delta\zeta=\Delta\zeta_{\exp i}*,\ \Delta A=\Delta A_{\exp i}*\right\} \tag{9}$$

The absolute values of these variations are now used as the best uncertainty bounds for that particular $E_i(j\omega)$. This reduces the bounds without modifying $F_k(j\omega)^b$ or increasing the value of the minimal error.

$$H(j\omega)_{\exp i}:=\left\{\frac{(A+\Delta A)}{(\omega_n+\Delta\omega_n)^2-\omega^2+2j(\zeta+\Delta\zeta)(\omega_n+\Delta\omega_n)\omega}: \left|\Delta\omega_n\right|\le\left|\Delta\omega_{n\ \exp i}*\right|,\ \left|\Delta\zeta\right|\le\left|\Delta\zeta_{\exp i}*\right|,\ \left|\Delta A\right|\le\left|\Delta A_{\exp i}*\right|\right\} \tag{10}$$

This entire procedure is repeated for all experimental responses $E_i(j\omega)$, $i=1,\dots,M$. The final best uncertainty bounds are defined as the maximum of the best uncertainty bounds over all experimental responses. This ensures the most similar model response, $F_k(j\omega)^b$, for each of the M experimental responses is included in the family of perturbed models $\mathcal{F}$.

This procedure may be applied to different models. However, when the number of parameters is large, it becomes very lengthy. As an example, a model with 10 modes is used, represented again by the receptance function. With 3 parameters per mode, there are 30 parameters in total.

$$H(j\omega)=\sum_{n=1}^{10}\frac{A_n}{\omega_n{}^2-\omega^2+2j\zeta_n\omega_n\omega} \tag{11}$$

Suppose all initial uncertainty bounds are of ±5%. In order to get a finite subset of $\mathcal{F}$, the bounds are discretized. If the increment used is 1%, this results in 11 possible values for each parameter. With 30 parameters and 11 values each, a total of $1.7449\text{x}10^{31}$ combinations are generated. Since

$F_k(j\omega)^b$ is found by trial and error, one may want to reduce the number of comparisons required. A way to simplify the problem is to divide the response in its different modes, or natural frequencies. Instead of varying all parameters simultaneously, only the parameters for a particular mode are varied at a time. The error is minimized over the whole frequency range. This procedure is then repeated for the next mode, keeping the selected parameters from the preceding mode. In this case, with 3 parameters per mode, the number of combinations for each minimization is reduced to 1331. This minimization is performed from the first mode to the last and then from the last mode to the first. This loop is repeated until the error converges.

Example

The car suspension has been modeled using 13 modes. Its modal model is a summation of 13 acceleration transfer functions.

$$H(j\omega)=\sum_{n=1}^{13}\frac{-A_n\omega^2}{\omega_n^{\ 2}-\omega^2+2j\zeta_n\omega_n\omega} \qquad (12)$$

Three experimental data sets are compared to the perturbed models defined by the uncertainty bounds. The starting maximum bounds are initially defined as very small values. For each experimental response, the most similar perturbed model $F_k(j\omega)^b$ is determined and the mean error is computed. The bounds are increased until the mean error reaches a minimum value. The bounds are then

$$\Delta\omega_{n\,\max}=1\%,\ \ \Delta\zeta_{\max}=1\%,\ \ \Delta A_{\max}=1\% \qquad (13)$$

for all 13 modes. The bounds are discretized using a 0.2% step. It is then attempted to reduce certain bounds while varying the step size, without increasing the error. Finally, the following maximum bounds are selected.

$$\begin{aligned}\Delta\omega_{n\,\max}&=1.0\% &&\text{step of } 0.02\ \%\\ \Delta\zeta_{\max}&=0.1\% &&\text{step of } 0.1\ \%\\ \Delta A_{\max}&=0.6\% &&\text{step of } 0.2\ \%\end{aligned} \qquad (14)$$

The most similar perturbed model $F_k(j\omega)^b$ is again determined for each experimental response. For simplicity, as the experimental responses do not vary much from one another, the maximum bounds are kept constant for all three responses. Figure 7 shows $F_k(j\omega)^b$ for the first experimental response.

The maximum absolute value over all experiments for each parameter are listed in Table 2 below, defining the best uncertainty bounds for the car suspension model.

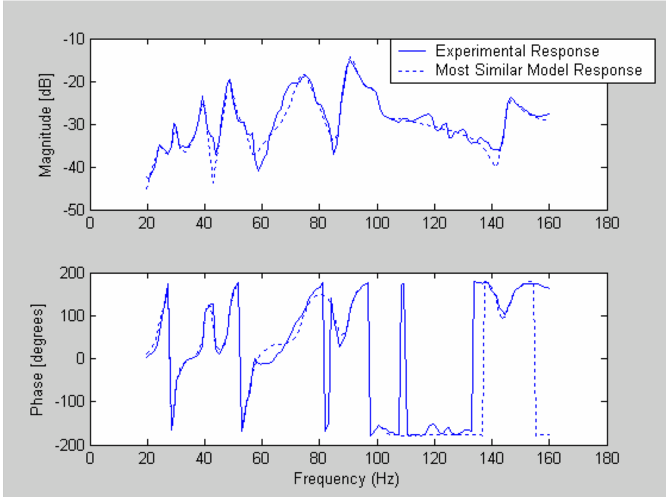

Figure 7: Most Similar Model Response for Experimental Response #1

Table 2: Best Uncertainty Bounds for Suspension Model

Mode	$\Delta\omega_{n\,\max}$	$\Delta\delta_{\max}$	$\Delta A_{\max}$
1	1.00 %	0.10 %	0.60 %
2	0.86 %	0.10 %	0.60 %
3	1.00 %	0.10 %	0.60 %
4	0.90 %	0.10 %	0.60 %
5	0.50 %	0.10 %	0.60 %
6	0.30 %	0.10 %	0.60 %
7	1.00 %	0.10 %	0.60 %
8	1.00 %	0.10 %	0.60 %
9	1.00 %	0.10 %	0.60 %
10	0.40 %	0.10 %	0.60 %
11	0.52 %	0.10 %	0.60 %
12	1.00 %	0.10 %	0.60 %
13	0.08 %	0.10 %	0.60 %

F. Model Limitations

The final model, as accurate as it is, still suffers from several limitations. Since it is based on experimental data, there is a certain amount of uncertainty due to noise or to physical limitations of the sensors. This uncertainty translates into FRFs that may contain some errors, as is evidenced by the coherence function. The next step, the curve-fitting process, also introduces uncertainty in the model, as it is impossible to exactly fit the FRF data. Due to the necessity of having a finite and manageable number of DOFs, certain modes have to be ignored, as well as the modes outside the frequency range of interest that may have an effect on the response in the frequency range of interest. This can lead to additional uncertainty on the modal parameters as well. Finally, the structure is assumed to be LTI, but some operating conditions may cause the structure to be time varying, such as temperature variations, or wear of the mechanical components. The suspension also contains such nonlinearities as saturations and nonlinear stiffness.

III. Preliminary Controller Design

We designed a state-feedback controller using the H_∞ technique and coupled it with a state observer. This preliminary controller design based on the nominal model of the suspension was not meant to meet any specific robustness or performance objective, however the results in **Figure 8** show that multivariable feedback control can work to reduce vibration at the suspension attachment points.

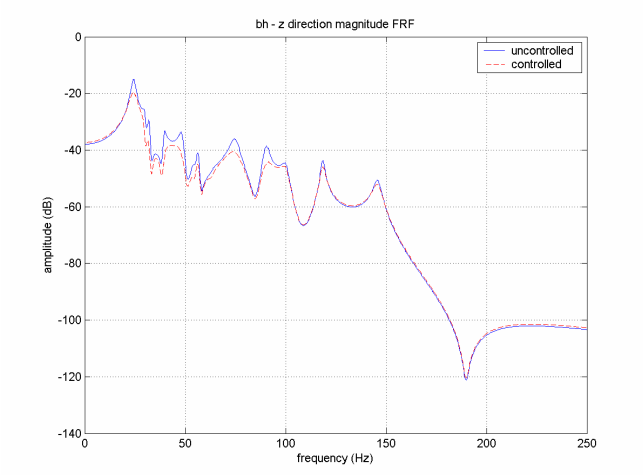

Figure 8 - bh, z direction closed-loop dB attenuation

The head sensors register an attenuation of the peaks below 100 Hz of about 5-8 dB. A new model was derived with random variations introduced on the modal parameters. The variations are of up to 10% on the modal frequencies and 40% on the damping ratios. The same controller is applied to this "randomized" model to see if it retains its performance. As shown in **Figure 9**, despite a model that is fairly different from the one used to derive the controller, the performance remains almost as good as when it was applied to the original model.

IV. Conclusion

While every effort has been made to model the car suspension testbed as accurately as possible, a completely accurate model is impossible to obtain. It is therefore important to know that the controller will perform well on the real system even if it differs from the model. Thus, the next logical step in this project will be to design robust mu-synthesis controllers for the uncertainty bounds obtained in this research and test them on the experimental testbed to assess their performance.

Developing a structural-acoustic FEM of a complete automobile will also take the project further. The global aim being to reduce the noise level inside the passenger cabin of the car, knowledge of the frequencies that produce the most noise will enable the tuning of the controller to reduce specifically those noise-generating resonances. Furthermore, using the FEM in the simulation will allow the use of microphones placed at strategic locations in the cabin to be used as the feedback signal to the controller. The ability to control directly the noise level will therefore improve controller performance.

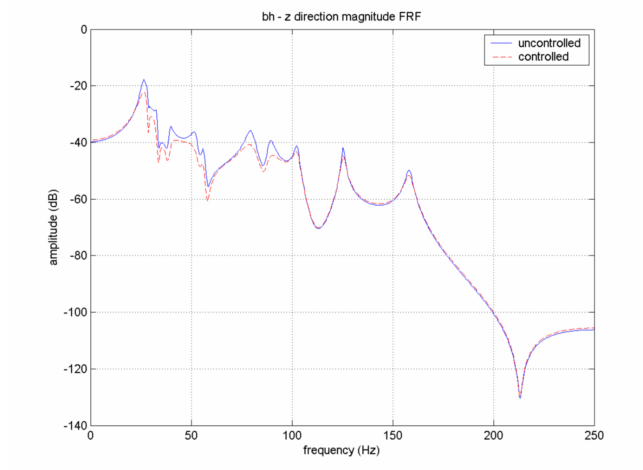

Figure 9 – bh, z direction closed-loop dB attenuation on randomized model

Acknowledgment

This research was supported by the AUTO21 Network of Centres of Excellence of Canada.

References

[1] Hermans, L. and Van Der Auweraer, H. (1999) 'Modal Testing and Analysis of Structures Under Operational Conditions : Industrial Applications', *Mechanical Systems and Signal Processing*, Vol 13, No 2, pp 193-216.

[2] Kim, S.H., Lee, J.M. and Sung, M.H. (1999) 'Structural-Acoustic Modal Coupling Analysis and Application to Noise Reduction in a Vehicle Passenger Compartment', *Journal of Sound and Vibration*, Vol 225, No 5, pp 989-999.

[3] Stobener, U. and Gaul, L. (2001) 'Active Vibration Control of a Car Body Based on Experimentally Evaluated Modal Parameters', *Mechanical Systems and Signal Processing*, Vol 15, No 1, pp 173-188.

[4] Kar, I.N., Seto, K. and Doi, F. (2000) 'Multimode Vibration Control of a Flexible Structure Using H_∞-Based Robust Control'. *IEEE/ASME Trans. Mechatronics*, Vol 5, No 1, pp 23-31.

[5] Boulet, B., Francis, B.A., Hughes, P.C. and Hong, T. (1997) 'Uncertainty Modeling and Experiments in H∞ Control of Large Flexible Space Structures', *IEEE Trans.Con.t. Syst. Tech.*, Vol 5, No 5, pp 504-519.

[6] Ewins, D.J. (2000) *Modal Testing: Theory, Practice and Application*, Research Study Press LTD.

[7] Ewins, D.J. (1984) *Modal testing : Theory and practice*, Research Studies Press LTD.

[8] He, J. and Fu, Z-F (2001) *Modal Analysis*, Butterworth-Heinemann, Oxford.

[9] The Mathworks Inc, *Curve Fitting Toolbox User's Guide*. http://www.mathworks.com

[10] The Mathworks Inc, *Control System Toolbox For Use With Matlab*. http://www.mathworks.com

[11] The Mathworks Inc, *Mu-Analysis and Synthesis Toolbox User's Guide*. http://mathworks.com